Excess entropy scaling for soft particle glasses

Roger T. Bonnecaze, Fardin Khabaz, Lavanya Mohan, Michel Cloitre

Excess Entropy Scaling for Soft Particle Glasses

Roger T. Bonnecaze[1*], Fardin Khabaz[1], Lavanya Mohan[1↓], Michel Cloitre[2]

[1]*McKetta Department of Chemical Engineering, The University of Texas at Austin, Austin, TX, 78712, USA*

[2]*Molecular, Macromolecular Chemistry, and Materials, ESPCI Paris, CNRS, PSL University, 10 Rue Vauquelin, 75005 Paris, France*

[*]Corresponding author electronic mail: rtb@che.utexas.edu

[↓]Current address: Exxon Mobil Upstream Research Company, 3120 Buffalo Speedway, Houston, TX 77098

Abstract

The transport properties of soft particle glasses, such as dynamic viscosity, normal stress coefficients, and shear-induced diffusivity of its particles, are determined by the microstructure of the suspension under flow. A thermodynamic measure of the microstructure is the excess entropy, which we show here accurately correlates the transport properties of soft particle glasses onto master curves across a wide range of volume fractions, suspending fluid viscosities, particle moduli and shear rates. The excess entropy for soft particle glasses is approximated with the two-body excess entropy computed from the pair distribution function extracted from dynamic simulations. The shear viscosity and normal stress functions diverge and the diffusivity vanishes at a critical excess entropy, corresponding to the yield stress of the suspension. An effective temperature is computed and is found to vary linearly with the shear stress and the elastic energy of the sheared soft particle glass. From this an equation of state is derived relating the excess entropy to the shear stress. Consequently, three of the four transport properties are determined from the measurement of just one. Finally, a single master curve of particle diffusivity versus excess entropy is presented that unifies observations for both equilibrium and non-equilibrium suspensions.

I. Introduction

In 1977 Rosenfeld proposed and showed for the first time that the diffusivity and viscosity of fluids composed of particles interacting with Lennard-Jones and short-ranged repulsive interparticle potentials are correlated onto a master curve as a function of the excess entropy of the system [1]. Separately, Dzugotov showed a similar correlation for liquid metals [2]. Many other studies have followed using excess entropy as a means to correlate the diffusivity and viscosity for a variety of atomic, molecular and colloidal systems, and interparticle potentials [3-17]. Truskett and co-workers have also shown how the correlation extends to particles in confined systems, thus connecting the properties in confinement to those in the bulk [8, 18]. In all these studies the systems were at equilibrium and there was no flow.

In Rosenfeld's and Dzugotov's original works, the normalized or so-called reduced diffusivity and viscosity were found to scale like $e^{\alpha S^E}$ and $e^{-\beta S^E}$, respectively, where S^E is the dimensionless excess entropy relative to that of an ideal gas on a per particle basis and normalized by the Boltzmann factor. Note the excess entropy is negative. The constants α and β are positive, typically about equal and around 0.65-0.95. The normalization for the diffusivity and viscosity is based on the characteristic length and time scales for the systems of interest. While these scalings are observed for moderate values of the excess entropy, the diffusivity increases according to $-1/S^E$ at low values [10]. In this paper we show that the diffusivity can also vanish as S^E approaches a value of the excess entropy S_y^E, corresponding to its value at the yield stress of the suspension. In general if the normalized dynamic properties of a material at different temperatures and pressures are determined by S^E, it is said to obey the excess entropy scaling [4]. The success of this scaling was initially argued to be based on the excess entropy being a measure of the free

volume available to the particles which is the underlying microstructural determinant for the transport properties of the system [1, 5, 12].

The excess entropy scaling does not always work [4, 19]. For example, systems of particles that interact with potentials with distinct directional bonding do not obey the excess entropy scaling. The exact requirement is that the interparticle potential be Euler homogeneous, i.e., $U(\lambda\mathbf{R}) = \lambda^{-n}U(\mathbf{R})$, where U is the potential energy for the system, $\mathbf{R}$ is the coordinates of the configuration and λ is a scaling factor [4]. In practice if this is approximately satisfied, the excess entropy scaling will collapse the dynamic properties of the system.

Here we explore the effectiveness of using the excess entropy to correlate transport properties of athermal, jammed suspensions activated by shear, specifically soft particles glasses (SPGs). SPGs are concentrated suspensions of deformable particles such as microgels, droplets, and micelles. The volume concentration of these suspensions is well above random close packing for spheres. The dominant forces for these materials are repulsive elastic or Hertzian-like interparticle interactions, which are typically much larger than thermal forces. At rest the suspension is in a trapped glassy state. Under shear flow, the particles become mobile and can diffuse. The shear and normal stresses for SPGs follow a Herschel-Bulkley form [20-22]. All previous examples of the excess entropy scaling are for quiescent, thermally equilibrated systems, except for a study on the shear viscosity of attractive particles with significant thermal forces [23-25]. This paper aims to answer the following questions. Does the excess entropy correlation work for a non-equilibrium, athermal, shear activated system to correlate diffusivity and the shear and normal stress viscosities of SPGs? Can one construct a temperature and an equation of state for the SPGs connecting rheological properties to excess entropy? Finally, is there a universal scaling with

excess entropy for diffusivity for colloidal systems regardless of whether they are thermally or shear activated?

II. Simulations Methods

The details of the model and the simulation method have been presented in previous studies [22, 26-30]. Here we briefly summarize the essential features. Soft particle glasses are modeled as suspensions of 10^4 non-Brownian elastic particles in a solvent with a viscosity of η_s that are jammed at volume fractions larger than the random close-packing of hard spheres. Suspensions with an average radius of unity scaled by the average radius R, polydispersity index of $\delta = 0.2$ [27, 28], and volume fractions of $\phi = 0.7, 0.75, 0.8, 0.85$, and 0.9 are studied. At contact between particles α and β, they create a flat facet resulting in a deformation of $\varepsilon_{\alpha,\beta} = 0.5\left(R_\alpha + R_\beta - r_{\alpha\beta}\right)\big/R_c$, where R_α and R_β are the radii of particle α and β, $r_{\alpha\beta}$ is the center-to-center distance, and R_c is the contact radius, which is given as $R_c = R_\alpha R_\beta \big/ \left(R_\alpha + R_\beta\right)$.

The elastic repulsion force between particles α and β acts perpendicularly to the contacting facet (*i.e.*, $\mathbf{n}_\perp$). It is given by the generalized Hertz law [30]:

$$\mathbf{f}^e_{\alpha\beta} = \frac{4}{3} C E^* \varepsilon^n_{\alpha\beta} R_c^2 \mathbf{n}_\perp , \tag{1}$$

where E^* is the particle contact modulus: $E^* = E\big/2\left(1-\nu^2\right)$, with E being the Young modulus and ν = 0.5 is the Poisson ratio. C and n are parameters, which depend on the degree of compression. For $\varepsilon < 0.1$ $n = 1.5$ and $C = 1$, for $0.1 \le \varepsilon < 0.2$ $n = 3$ and $C = 32$, and if $0.2 \le \varepsilon < 0.6$ $n = 5$ and $C = 790$ [30, 31]. The elastohydrodynamic (EHD) drag force, which is due to the existence of

thin films of solvent between the flat facets of two particles in contact during the shear deformation [30], is parallel to the contacting facets and is given by:

$$\mathbf{f}_{\alpha\beta}^{\mathrm{EHD}} = -\left(\eta_s C u_{\alpha\beta,\parallel} E^* R_c^3\right)^{1/2} \varepsilon_{\alpha\beta}^{(2n+1)/4} \mathbf{n}_{\parallel}, \tag{2}$$

where $u_{\alpha\beta,\parallel}$ is the relative velocity component in the direction of parallel to the contacting facets (*i.e.*, $\mathbf{n}_{\parallel}$). The fluid inertia is neglected, and the forces are assumed to be pair-wise additive. The velocity field due to the motion of the solvent is given as $\mathbf{u}_{\alpha}^{\infty} = \frac{\dot{\gamma}\eta_s}{E^*} y\mathbf{e}_x$, where $\mathbf{e}_x$ is the basis vector in the x-direction. The resulting equation of motion is made dimensionless by scaling lengths, time and velocity by R, $\dot{\gamma}^{-1}$ and $\dot{\gamma}R$ respectively, leading to [29, 30]:

$$\frac{d\tilde{\mathbf{x}}_{\alpha}}{d\tilde{t}} = \tilde{\mathbf{u}}_{\alpha}^{\infty} + \frac{M}{\tilde{R}_{\alpha}}\left[\frac{4}{3} C\tilde{\dot{\gamma}}^{-1} \sum_{\beta} \varepsilon_{\alpha\beta}^{n} \tilde{R}_c^2 \mathbf{n}_{\perp} - \tilde{\dot{\gamma}}^{-1/2} \sum_{\beta} \left(C\tilde{u}_{\alpha\beta,\parallel} \tilde{R}_c^3\right)^{1/2} \varepsilon_{\alpha\beta}^{(2n+1)/4} \mathbf{n}_{\parallel}\right], \tag{3}$$

where the tilde quantities are dimensionless variables. M is the mobility function which is that of a particle corrected by a factor $f(\phi)$ that accounts for its reduction at high volume fraction, namely $M = f(\phi)/6\pi$; $f(\phi)$ is set to 0.01 in the simulations. $\mathbf{x}_{\alpha}$ is the position of the particle α. The form of this equation shows that the dynamics is characterized by the dimensionless shear rate $\tilde{\dot{\gamma}} = \dot{\gamma}\eta_s / E^*$, which represents the ratio of viscous to elastic forces, and the overlap deformation that depends on the volume fraction. The Lees-Edwards [32] boundary conditions are then used in the LAMMPS package [33] in order to impart the desired shear rate to the simulation box.

Given the position of the particles at any instant in time, the stress, elastic energy, and entropy of the SPG under shear can be computed. The stress tensor of the suspensions is determined using the Kirkwood formula [34]:

$$\boldsymbol{\sigma} = \frac{1}{V}\sum_{\beta}^{N}\sum_{\alpha>\beta}^{N}\mathbf{f}_{\alpha\beta}\left(\mathbf{x}_{\alpha}-\mathbf{x}_{\beta}\right), \tag{4}$$

where V is the volume of the system and $\mathbf{f}_{\alpha\beta} = \mathbf{f}_{\alpha\beta}^{e} + \mathbf{f}_{\alpha\beta}^{EHD}$ is the total force acting on particle α from particle β. The shear stress σ_{xy}, the first and second normal stress differences, $N_1 = \sigma_{xx} - \sigma_{yy}$ and $N_2 = \sigma_{yy} - \sigma_{zz}$, are computed from the appropriate components of the stress tensor. The dimensionless average elastic energy per volume of the SPGs is determined from the pairwise interaction energy between particles according to

$$U = \frac{8}{3N}\sum_{\alpha=1}^{N}\sum_{\beta>\alpha}^{N}\frac{C\varepsilon_{\alpha\beta}^{n+1}R_c^3}{(n+1)}, \tag{5}$$

where the C and n parameters are those used in the force law in Eq. (1). The elastic energy here is non-dimensionalized by E^*R^3.

The excess entropy of the SPGs is approximated by determining the two-body contribution to the entropy as follows[3]:

$$S^E \cong S_2 = -\frac{1}{2}\rho\int\left[g(\mathbf{r})\ln\left(g(\mathbf{r})\right) - g(\mathbf{r}) + 1\right]d\mathbf{r}, \tag{6}$$

where S^E is the dimensionless excess entropy per particle, $g(\mathbf{r})$ is the pair distribution function between the particles that is determined in a steady-state flow condition, and ρ is the number density of the SPGs. The excess entropy is non-dimensionalized by the Boltzmann factor k_B. The temperature T is calculated from the derivative of the energy with respect to the excess entropy, *i.e.*, $T = \left(dU/dS^E\right)_{N,V}$. The temperature reported here is non-dimensionalized by E^*R^3/k_B. Eqn. (6) has been used successfully to compute the excess entropy for liquids. SPGs are certainly not

typical liquids in that they are shear rather than thermally activated. That being said, they have a pair distribution functions that shows no long range order and approaches unity around three particle diameters from the reference particle, similar to other liquids[20, 35].

The flow properties and microstructure of the suspensions were investigated over a broad range of shear rates ranging from $\tilde{\dot{\gamma}}=10^{-9}$ to $\tilde{\dot{\gamma}}=10^{-4}$. The simulations were performed for 100 strain units, and the stress tensor is calculated at regular strain intervals. The value of the time step was chosen such that it produced 10^7 steps per strain at each shear rate.

II. Results

II. A. Overview of rheology and dynamics of SPGs

The steady-state dimensionless shear stress σ/E^* is plotted against the dimensionless shear rate $\dot{\gamma}\eta_s/E^*$ in Fig. 1a. Suspensions show a yield behavior at very low shear rates, and then by increasing the shear rate they start flowing. The magnitude of the yield stress σ_y/E^* increases with the volume fraction of suspensions. Similarly, the first and second normal stress differences (N_1/E^* and $-N_2/E^*$) are plotted as a function of the shear rate in Fig. 1b and Fig. 1c for SPGs with different volume fractions. At low shear rates, a similar yield behavior as seen in Fig. 1a is observed for normal stress differences in Fig. 1b and Fig. 1c. This yield behavior is followed-up by the power-law increase of the shear stress at high shear rates (*i.e.*, shear thinning regime). The shear rate is rescaled using the low-frequency modulus G_0 of these pastes, i.e., $\dot{\gamma}\eta_s/G_0$ [26, 36]. The rescaled shear stress σ/σ_y collapse onto a master curve, and they follow the Herschel-Bulkley (HB) relationship with an exponent of 0.48 for the shear stress as seen in Fig.1 d (σ_y is obtained from fitting the individual shear stress data in Fig. 1a to the HB relationship). The normalized

stress differences also show a universal trend as a function of the shear rate $\dot{\gamma}\eta_s/G_0$ as seen in Fig. 1e and Fig. 1f.

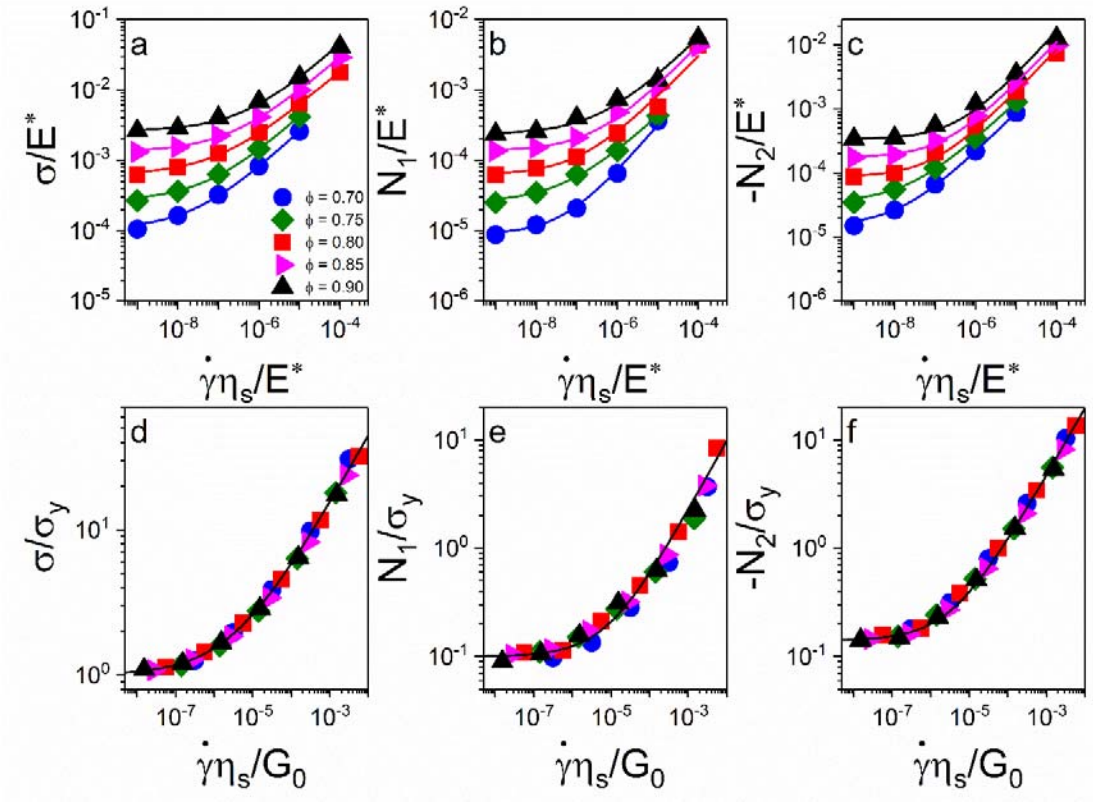

FIG 1. (a) Shear stress σ/E^*, (b) first N_1/σ_y, and (c) second normal stress differences $-N_2/\sigma_y$ as a function of the shear rate $\dot{\gamma}\eta_s/E^*$. Rescaled (d) shear stress σ/σ_y, (e) first N_1/σ_y, and (f) second normal stress differences $-N_2/\sigma_y$ as a function of the rescaled shear rate $\dot{\gamma}\eta_s/G_0$. The lines in (d-f) are the best fits of the data to the Herschel-Bulkley (HB) equation: $\sigma/\sigma_y = 1+404\left(\dot{\gamma}\eta_s/G_0\right)^{0.48\pm0.02}$, $N_1/\sigma_y = 0.1+195\left(\dot{\gamma}\eta_s/G_0\right)^{0.65\pm0.02}$, $-N_2/\sigma_y = 0.14+359\left(\dot{\gamma}\eta_s/G_0\right)^{0.63\pm0.02}$.

The shear induced diffusion coefficient of the suspensions is determined from the diffusive part of the mean-squared displacement of the SPGs [22] at different shear rates to characterize the dynamics of SPGs. As seen in Fig. 2, the diffusion coefficient data collapse onto a master curve. At low shear rates, the rescaled diffusion coefficient $D\eta_s/G_0R^2$ follows a linear relationship as a function of the shear rate, while at high shear rates (where stress increases in a power-law fashion),

we observe a power-law relationship between the $D\eta_s/G_0R^2$ and $\dot{\gamma}\eta_s/G_0$ with an exponent of $2/3$. The crossover between the low and high shear regimes is determined from the intersection between the power-law behaviors at low and high shear rates, around $\dot{\gamma}\eta_S/G_0 \cong 5\times10^{-6}$, as noted by Khabaz et al.[37]. It is important to note that this value is the same as the one that marks the crossover between the low shear plateau and the power law regime for the stress and normal stress differences in Fig. 1d.

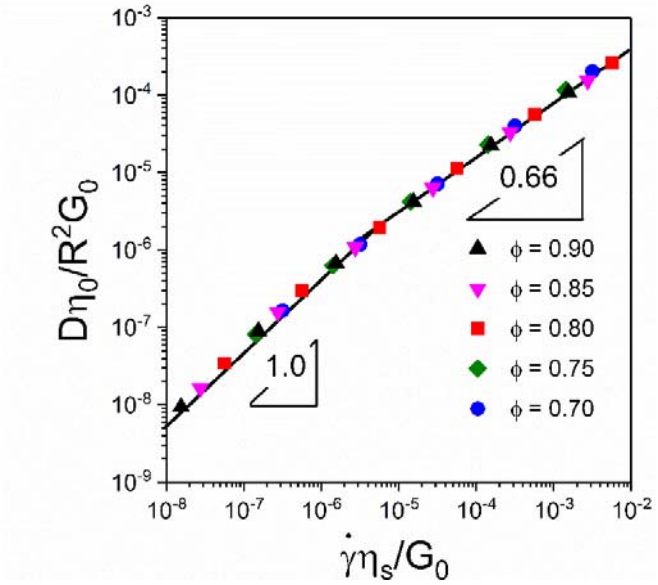

FIG 2. The diffusion coefficient $D\eta_s/G_0R^2$ as a function of the rescaled shear rate $\dot{\gamma}\eta_s/G_0$.

The elastic energy U of the SPGs at different volume fractions is determined using Eq. (6) at different shear rates $\dot{\gamma}\eta_s/E^*$. As seen in Fig. 3a, at low shear rates, the elastic energy shows a yield value, and then it increases in a power-law fashion according to the HB relationship (elastic energy data in each volume fraction are fitted to the HB relationship $U = U_y + k\left(\eta_s\dot{\gamma}/E^*\right)^n$ and the yield value of the elastic energy U_y is extracted). The yield value of the elastic energy U_y

increases with the volume fraction of suspensions. Using the rescaled shear rate $\dot{\gamma}\eta_s/G_0$, all elastic energy data collapse onto a master curve as demonstrated in Fig. 3b.

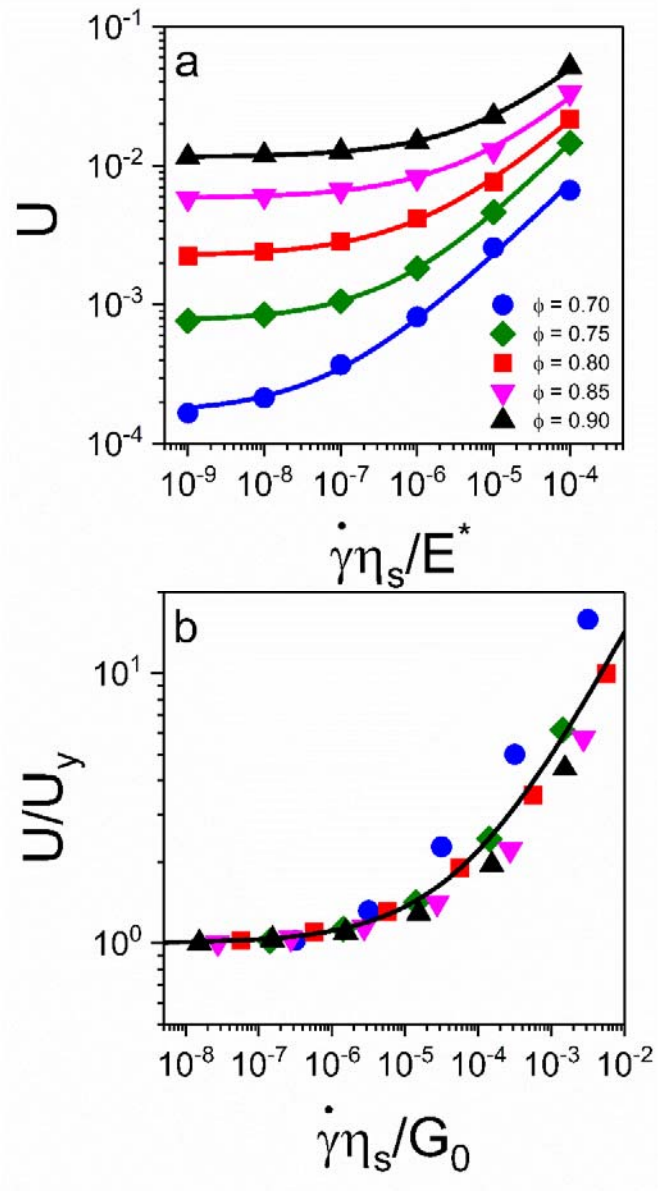

FIG 3. (a) Elastic energy U as a function of shear rate $\dot{\gamma}\eta_s/E^*$ and (b) master curve of the rescaled elastic energy U/U_y as a function of the rescaled shear rate $\dot{\gamma}\eta_s/G_0$ for SPGs with different volume fractions. The solid lines in (a) shows the HB equation fit to data given by $U = U_y + k\left(\eta_s\dot{\gamma}/E^*\right)^n$. The solid line in (b) shows the HB equation fit to data given by $U/U_y = 1 + 145\left(\eta_S\dot{\gamma}/G_0\right)^{0.52}$.

II. B. Excess entropy of SPGs and connection with macroscopic properties

The pair distribution function between the soft particles is computed and then used to calculate the excess entropy according to Eq. (6). The values of $-S^E$ are plotted against the shear rate for SPGs with different volume fractions in Fig. 4a. At low shear rates the values of $-S^E$ plateaus around a value of 9.0. As the shear rate increases the excess entropy increases (*i.e.*, $-S^E$ becomes less negative) due to the effect of shear flow, and it decreases with the volume fraction in the shear thinning part of the flow curve. Similar to the previous section, all excess entropy data collapse onto a master curve when plotted against the rescaled shear rate $\dot{\gamma}\eta_s/G_0$. The agreement is less good for $\phi = 0.7$ and the lowest shear rates. The poorer agreement here is unknown at this time. It may be that the two-body approximation to the excess entropy may be less accurate for these conditions. It is also that the excess entropy scaling fails under these conditions. It is has been noted that systems that become non-ergodic fail the entropy scaling and show lower than expected diffusivities compared to the ergodic systems where the scaling works[38].

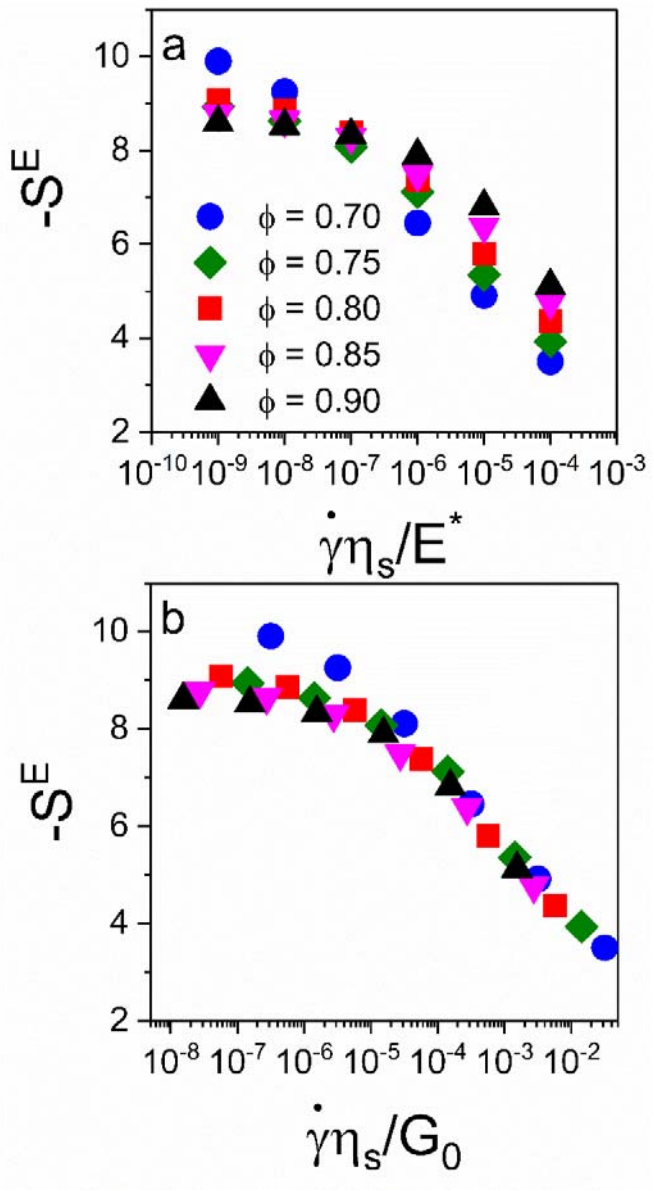

FIG 4. (a) Excess entropy $-S^E$ as a function of shear rate $\dot{\gamma}\eta_s/E^*$ for SPGs with different volume fractions. (b) Master curve of $-S^E$ as a function of the rescaled shear rate $\dot{\gamma}\eta_s/G_0$.

Using the elastic energy and the excess entropy we can define a "temperature" of the sheared suspension based on the thermodynamic relationship $T=\left(dU/dS^E\right)_{N,V}$. The values of the elastic energy U as a function of $-S^E$ are fitted to a power-law relationship, and then the temperature T is extracted (see Fig. S1 for U vs. $-S^E$). The values of the temperature T at

different volume fractions and shear rates are shown in Fig. 5. The temperature T at low shear rates near the yield stress is constant for a given volume fraction and is denoted by T_y. As the shear rate increases the temperature of the SPGs increases based on the HB relationship. Furthermore, temperature increases with an increase in the volume fraction of the suspensions. Using the normalized values of the temperature with respect to the yield temperature (*i.e.*, T/T_y) and the rescaled shear rate of $\dot{\gamma}\eta_s/G_0$, a master curve of the temperature is constructed in Fig. 5b. As seen in the figure, the T/T_y values follow the HB equation with an exponent of 0.5. The transition temperature between the quasi-static and shear thinning regimes occurs at a shear rate of $\dot{\gamma}\eta_s/G_0 \cong 5\times10^{-6}$ in agreement with our previous findings for the flow curves and cage relaxation time in these jammed suspensions [22].

We relate the elastic energy U and shear stress σ/E^* to the temperature T in Fig. 6a and Fig. 6b, respectively. As seen in Fig. 6a, the elastic energy shows a universal behavior for all the SPGs with different volume fractions, and it increases linearly with the temperature as $U = (1.65 \pm 0.10)T$. The shear stress also exhibits a universal linear trend as a function of the temperature as $\sigma = (1.31 \pm 0.05)T$ as seen in Fig. 6b. The linear relationships between energy, stress and temperature of SPGs was anticipated in earlier studies [21, 27, 39]. Mohan and Bonnecaze [39] used energy as a surrogate for temperature in the expression $-U\nabla \ln g(\mathbf{r})$ for the effective non-equilibrium elastic force acting on a particle in a SPG, analogous to a Brownian force [39]. Suspensions of SPGs under sufficiently high shear will transition from a glass microstructure to a layered one at sufficiently high shear rates [21, 27]. The transition is an activated process following an Arrhenius behavior if one uses stress rather than temperature[21].

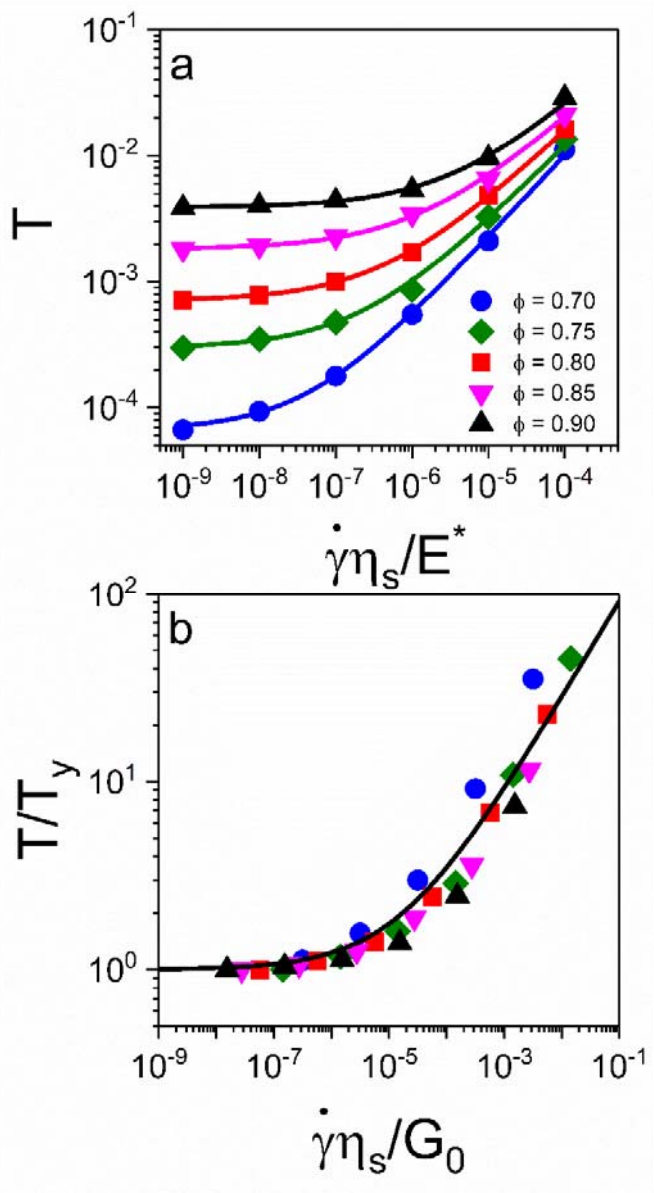

FIG 5. (a) Temperature T as a function of the shear rate $\dot{\gamma}\eta_s/E^*$ and (b) master curve of the rescaled temperature T/T_y as a function of the rescaled shear rate $\dot{\gamma}\eta_s/G_0$ for SPGs with different volume fractions. The solid lines in (a) shows the HB equation fit to data given by $T = T_y + k\left(\eta_s\dot{\gamma}/E^*\right)^n$. The solid line in (b) shows the HB equation fit to data given by $T/T_y = 1 + 301\left(\eta_S\dot{\gamma}/G_0\right)^{0.52}$.

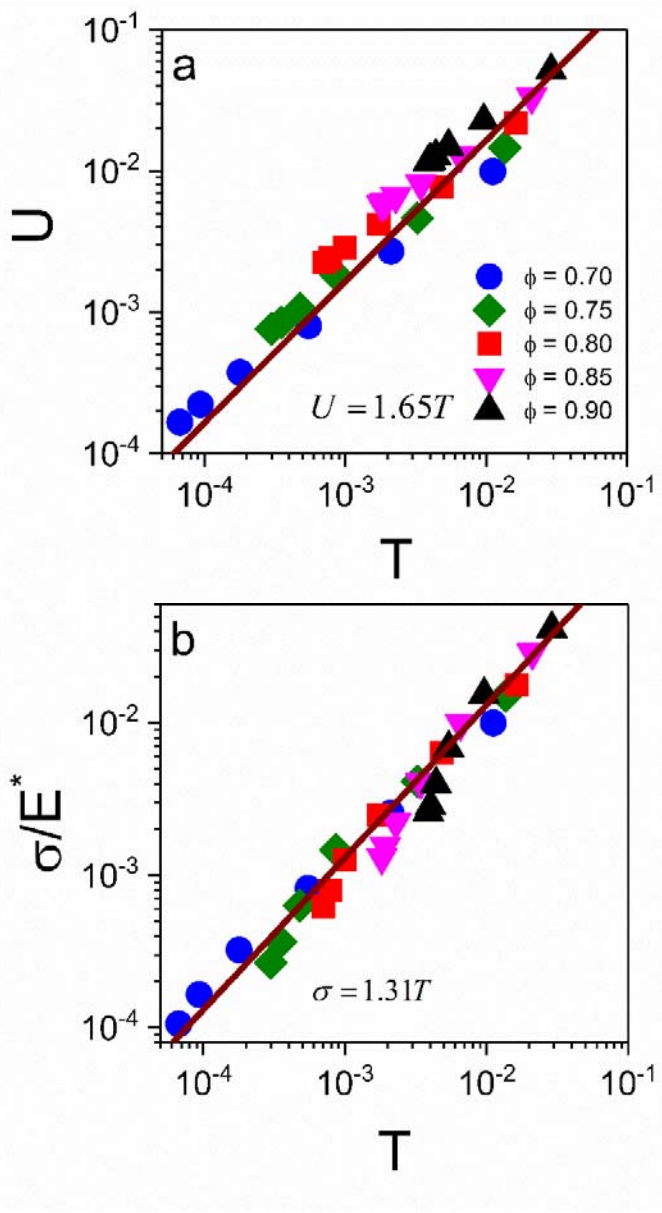

FIG 6. (a) Elastic energy U and (b) shear stress σ/E^* as a function of temperature T for SPGs with different volume fractions. The solid lines are the linear fit to data.

In order to establish a connection between the dynamics of SPGs and the excess entropy, the rescaled diffusion coefficient values are plotted against $-S^E$ in Fig. 7a. The diffusion coefficient increases with an increase in the excess entropy of the SPGs. A universal exponential correlation between the diffusion coefficient and the excess entropy, *i.e.*, $D\eta_s/R^2G_0 \sim \exp\left(\alpha S^E\right)$

is observed at low values of $-S^E$ with $\alpha \cong 1.1$, slightly higher than the value of 1.0 that is typically seen. At low shear rate and excess entropy, which corresponds to the quasi-static regime, the diffusion coefficient exhibits a sharp downward turn due to the solid-like nature of SPGs in this regime.

The rheology of SPGs is also correlated with the excess entropy by determining three viscometric functions, namely the shear viscosity, first and second normal stress coefficients. The shear viscosity is defined as the ratio of yielding part of the shear stress to the shear rate as $\eta_d = \left(\sigma - \sigma_y\right)/\dot{\gamma}$, and the first and second normal stress differences are defined as: $\psi_1 = N_1/\dot{\gamma}^2$ and $\psi_2 = N_2/\dot{\gamma}^2$, respectively. The rescaled shear viscosity with respect to the solvent viscosity η_d/η_s is plotted as a function of $-S^E$ in Fig. 7b. The shear viscosity increases with a decrease in the excess entropy. At large S^E, the shear viscosity decreases (shear thinning behavior) and shows an exponential decay with respect to S^E as $\eta_d \sim \eta_s \exp\left(-\beta S^E\right)$, where $\beta = \alpha \cong 1.1$. At smaller excess entropy that corresponds to yield behavior, the viscosity significantly increases and deviates from the exponential variation at high shear rates The first and second normal stress coefficients show the same behavior as a function of the S^E. Note that the transition from the quasi-static regime to the shear-thinning occurs at the same excess entropy (close to $-S^E \cong 9$) or equivalently the same shear rate in all of the macroscopic properties.

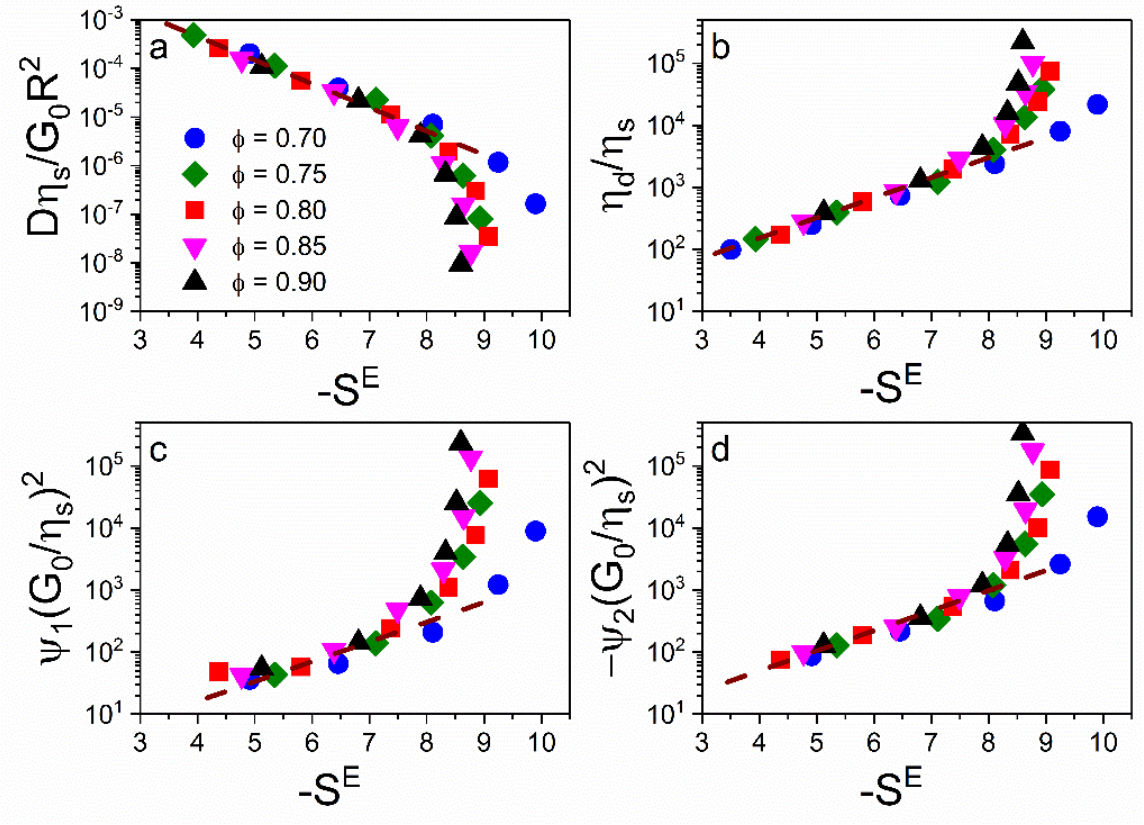

FIG 7. Master curve of (a) diffusion coefficient $D\eta_s/G_0R^2$, (b) shear viscosity, (c) first, and (d) second normal stress coefficient as a function of the $-S^E$. The dashed lines show the linear fits to data at large values of S^E.

IV. Discussion

The shear induced diffusivity, dynamic viscosity and normal stress coefficients for different volume fractions and shear rates collapse onto master curves of the excess entropy. However, the excess entropy thus far has been determined from detailed measurements of the microstructure, which are not often convenient or easily accessible. Expression of the excess entropy in terms of other more easily measurably quantities through an equation of state would be useful.

An equation of state relating the easily measurable shear stress to the excess entropy can be constructed from the observations in Fig. 6 that the energy and shear stress are linearly proportional to the temperature according to $U = 1.65T$ and $\sigma = 1.31T$. From that and $\left(dU/dS^E\right)_{N,V} = T$, we find that $1.65\left(d\sigma/dS^E\right)_{N,V} = \sigma$, which after integration becomes the equation of state,

$$-S^E = -S_y^E - B\ln\frac{\sigma}{\sigma_y}, \tag{7}$$

where B is a constant and $-S_y^E$ is the excess entropy at the yield point. Thus, the excess entropy can be determined from the shear stress flow curve. Indeed the shear stress follows the prediction of eqn. (7) as shown in Fig. 8. Based on the fit to data $-S_y^E$ is 9.8 ± 0.07 and B is 1.35 ± 0.09, which is close to 1.65 ± 0.10 that can be obtained from the relationships among U, σ and T. We should note that the linear fits in Fig. 6 are not perfect given that it covers almost three orders of magnitude of the data, but this form had the highest R^2 values of many tested. Considering these uncertainties, the value are of B consistent.

Figure 7 shows that the diffusivity and normal stress coefficients follow the excess entropy scaling. Thus, from eqn. (7) we can expect these dynamical properties to fall onto a master curve of the shear stress normalized by the yield stress. In Fig. 9a the diffusion coefficient $D\eta_s/R^2G_0$ is plotted as a function of the shear stress σ/σ_y. The diffusion coefficients of SPGs increase with the applied shear stress and show a universal behavior. Furthermore, the first and second normal stress coefficients, $\Psi_1(G_0/\eta_s)^2$ and $-\Psi_2(G_0/\eta_s)^2$, plotted against the shear stress in Fig. 9b and Fig. 9c also show the collapse onto a master curve. Thus, from the measurement of the shear stress flow curve, the shear diffusivity and the two normal stresses can be determined. Remarkably, the

measurement of any one of the four dynamical properties (i.e., diffusivity, shear stress or viscosity, and first and second normal stress coefficients) allows one to determine the other three.

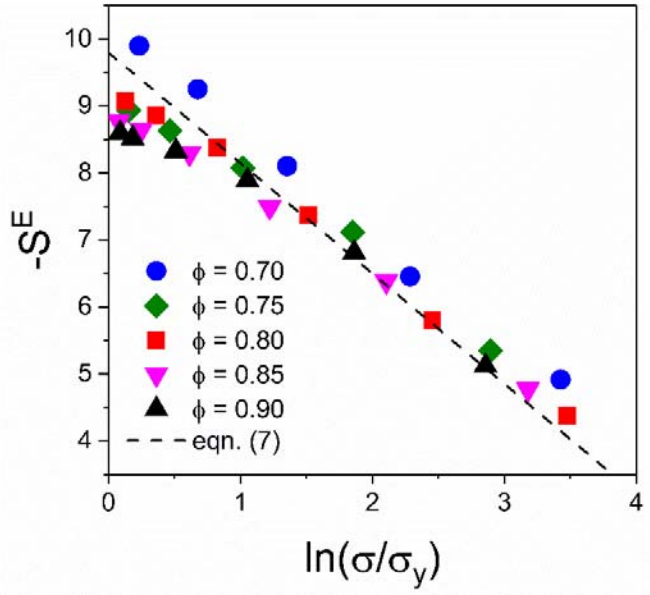

FIG 8. Master curve of the excess entropy $-S^E$ as a function of the shear stress $\ln\left(\sigma/\sigma_y\right)$. The best fit using eqn. (7) to data is shown by the dashed line.

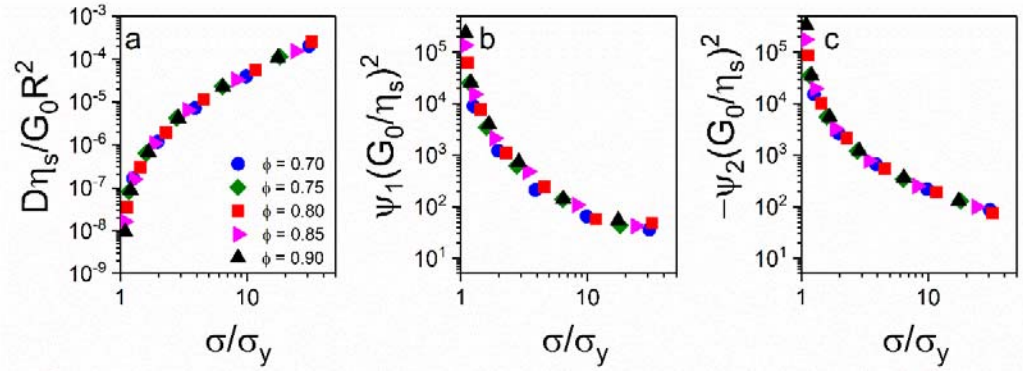

FIG 9. (a) Diffusion coefficient $D\eta_s/R^2G_0$, (b) first normal stress difference $\Psi_1\left(G_0/\eta_s\right)^2$, and (c) second normal stress difference $-\Psi_2\left(G_0/\eta_s\right)^2$ as a function of shear stress σ/σ_y obtained for SPGs with different volume fractions.

This interrelationship among the transport coefficients was also found by relating them to the microstructural relaxation time for the SPG [22]. This is the time required for a particle to escape a cage of surrounding particles when the suspension is sheared. Indeed the microstructural relaxation time for SPGs at different concentrations and shear rates versus the excess entropy all collapse onto a single master curve (see Fig. S2 in Supplementary Materials). Similar results for microstructural relaxation times have been observed for equilibrium [8] and sheared Brownian suspensions [24].

In order to compare the results of current simulations of SPGs with other systems, such as mono- and bi-dispersed suspensions of hard-spheres, metallic glasses, and Gaussian core fluids [1, 7, 9-11, 13, 19], the generalized diffusion coefficient D^*, which was proposed by Dzugutov [2], is determined as follows:

$$D^* = \frac{D_i}{\chi_i}, \tag{7}$$

where χ_i is the scaling factor, which is defined as:

$$\chi_i = 4\left(\pi k_B T\right)^{1/2} \sum_{j=1}^{N_c} x_i \rho \sigma_{ij}^4 g_{ij}\left(\sigma_{ij}\right)\left(\frac{m_i + m_j}{m_i m_j}\right)^{1/2}, \tag{8}$$

where k_B is the Boltzmann constant, x_i is the mole fraction of component *i*, $g_{ij}\left(\sigma_{ij}\right)$ is the magnitude of the pair distribution function between particles *i* and *j* determined at the contact, and m_i is the mass of particle *i*. Note that in our case the system of interest is a single component, thus $\chi = R^2 G_0 / \eta_s$. The generalized diffusion coefficient D^* for mono- and bidisperse hard spheres, liquid metals, and SPGs are plotted against $-S^E$ for various systems in Fig. 10. There appears a master curve that includes both the athermal and equilibrium systems. This means that

measurements or predictions of diffusivity from an equilibrium system can be used to predict that in an athermal non-equilibrium system at the same excess entropy and vice-versa, provided that that both follow the excess entropy scaling. Similar results are expected for viscosity and other transport properties.

The master curve for diffusivity breaks down for bidisperse hard spheres at moderate to low values of the excess entropy. The deviation occurs even before the diffusivity of the SPGs drops dramatically. The deviation may in part be due to the choice of the scaling for diffusivity. The collapse of data for molecular systems has been found to be sensitive to the choice of scaling[16], and this may explain the deviation seen with the bidisperse hard spheres.

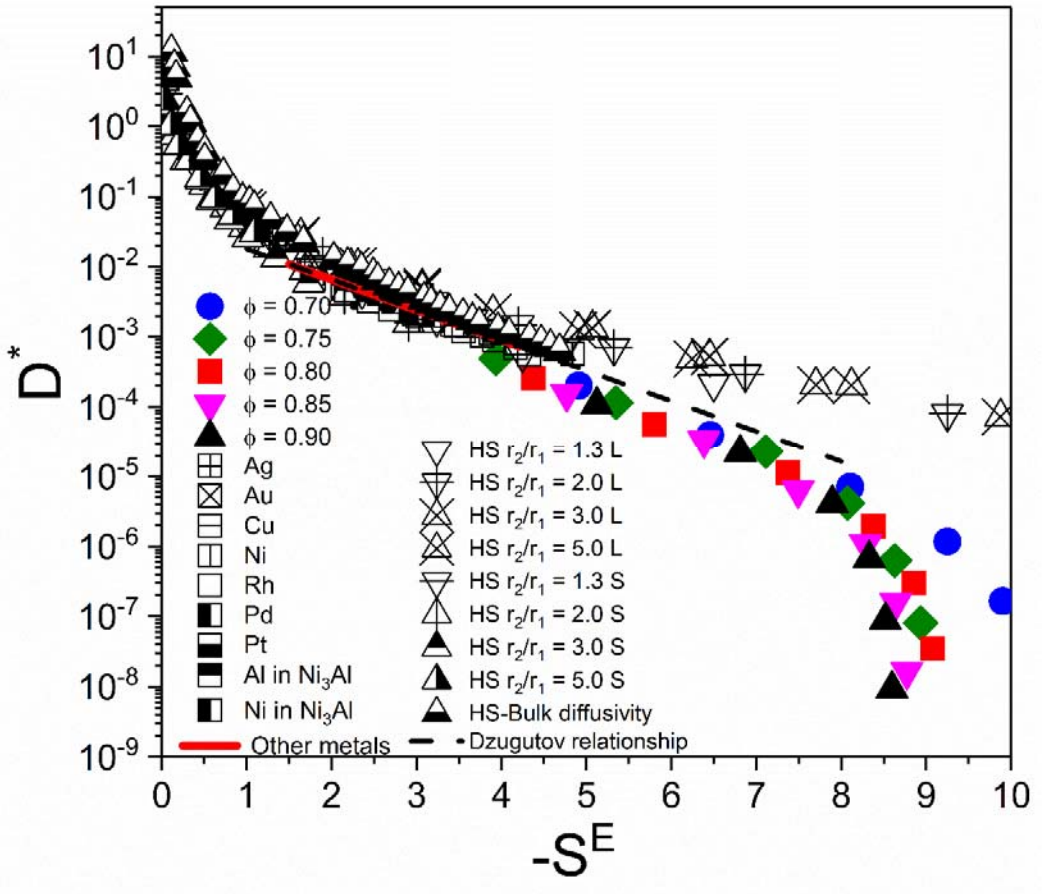

FIG 10. The generalized diffusion coefficient D^* obtained in current simulations of SPGs (filled symbols), metals (square and red line) [7, 11], and hard spheres (open and half-filled triangles) [10, 18], as a function of $-S^E$ for different systems.

V. Conclusions

We have shown that the shear-induced diffusivity, dynamic viscosity and first and second normal stress coefficients obey an excess entropy scaling. To the best of our knowledge, this is the first time such a scaling has been demonstrated for system that is shear activated with negligible thermal forces. At moderate values of the excess entropy, the normalized diffusivity and viscosity scales like $e^{\alpha S^E}$ and $e^{-\alpha S^E}$, as observed originally by Rosenfeld, Dzugotov and others. At larger values of the excess entropy, near the yielding the stress of the SPGs, the diffusivity approaches zero and the viscosity and normal stress coefficients approach infinity as $-S^E$ approaches a finite value. Interestingly, suitably normalized diffusivities from a variety of equilibrium thermal and the athermal sheared SPG system presented here collapse on a universal curve for excess entropy. This provides an intriguing connection between equilibrium and non-equilibrium and a possible means to predict properties of one from the other.

An effective temperature can also be derived for this sheared system from the computed relationship between elastic energy and excess entropy. For the SPGs the temperature scales linearly with both the shear stress and elastic energy. An equation of state can then be derived to predict the excess entropy from measurements of shear stress. This equation of state then allows one to predict any transport property (e.g., shear induced diffusivity or normal stresses) from the measurement of another (e.g., the shear stress).

Supplementary materials

See supplementary material for supporting information discussed in the main text.

Acknowledgments

FK and RTB gratefully acknowledge partial financial support from the National Science Foundation (MRSEC under award number DMR-1720595).

References

1. Rosenfeld, Y., *Relation between the Transport Coefficients and the Internal Entropy of Simple Systems.* Physical Review A, 1977. **15**(6): p. 2545.
2. Dzugutov, M., *A Universal Scaling Law for Atomic Diffusion in Condensed Matter.* Nature, 1996. **381**(6578): p. 137-139.
3. Baranyai, A. and D.J. Evans, *Direct Entropy Calculation from Computer Simulation of Liquids.* Physical Review A, 1989. **40**(7): p. 3817.
4. Dyre, J.C., *Perspective: Excess-Entropy Scaling.* The Journal of Chemical Physics, 2018. **149**(21): p. 210901.
5. Grover, R., W.G. Hoover, and B. Moran, *Corresponding States for Thermal Conductivities Via Nonequilibrium Molecular Dynamics.* The Journal of Chemical Physics, 1985. **83**(3): p. 1255-1259.
6. Guan, P., M. Chen, and T. Egami, *Stress-Temperature Scaling for Steady-State Flow in Metallic Glasses.* Physical Review Letters, 2010. **104**(20): p. 205701.
7. Hoyt, J., M. Asta, and B. Sadigh, *Test of the Universal Scaling Law for the Diffusion Coefficient in Liquid Metals.* Physical review letters, 2000. **85**(3): p. 594.
8. Ingebrigtsen, T.S., J.R. Errington, T.M. Truskett, and J.C. Dyre, *Predicting How Nanoconfinement Changes the Relaxation Time of a Supercooled Liquid.* Physical Review Letters, 2013. **111**(23): p. 235901.
9. Krekelberg, W.P., T. Kumar, J. Mittal, J.R. Errington, and T.M. Truskett, *Anomalous Structure and Dynamics of the Gaussian-Core Fluid.* Physical Review E, 2009. **79**(3): p. 031203.
10. Krekelberg, W.P., M.J. Pond, G. Goel, V.K. Shen, J.R. Errington, and T.M. Truskett, *Generalized Rosenfeld Scalings for Tracer Diffusivities in Not-So-Simple Fluids: Mixtures and Soft Particles.* Physical Review E, 2009. **80**(6): p. 061205.
11. Li, G., C. Liu, and Z. Zhu, *Excess Entropy Scaling for Transport Coefficients: Diffusion and Viscosity in Liquid Metals.* Journal of non-crystalline solids, 2005. **351**(10-11): p. 946-950.
12. Rosenfeld, Y., *Excess-Entropy and Freezing-Temperature Scalings for Transport Coefficients: Self-Diffusion in Yukawa Systems.* Physical Review E, 2000. **62**(5): p. 7524-7527.
13. Vaz, R.V., A.L. Magalhães, D.L.A. Fernandes, and C.M. Silva, *Universal Correlation of Self-Diffusion Coefficients of Model and Real Fluids Based on Residual Entropy Scaling Law.* Chemical Engineering Science, 2012. **79**: p. 153-162.
14. Rosenfeld, Y., *A Quasi-Universal Scaling Law for Atomic Transport in Simple Fluids.* Journal of Physics: Condensed Matter, 1999. **11**(28): p. 5415-5427.
15. Lötgering-Lin, O., M. Fischer, M. Hopp, and J. Gross, *Pure Substance and Mixture Viscosities Based on Entropy Scaling and an Analytic Equation of State.* Industrial & Engineering Chemistry Research, 2018. **57**(11): p. 4095-4114.
16. Hopp, M., J. Mele, and J. Gross, *Self-Diffusion Coefficients from Entropy Scaling Using the Pcp-Saft Equation of State.* Industrial & Engineering Chemistry Research, 2018. **57**(38): p. 12942-12950.
17. Ma, X., J. Liu, Y. Zhang, P. Habdas, and A.G. Yodh, *Excess Entropy and Long-Time Diffusion in Colloidal Fluids with Short-Range Interparticle Attraction.* The Journal of Chemical Physics, 2019. **150**(14): p. 144907.

18. Mittal, J., J.R. Errington, and T.M. Truskett, *Thermodynamics Predicts How Confinement Modifies the Dynamics of the Equilibrium Hard-Sphere Fluid.* Physical Review Letters, 2006. **96**(17): p. 177804.
19. Fomin, Y.D., V. Ryzhov, and N. Gribova, *Breakdown of Excess Entropy Scaling for Systems with Thermodynamic Anomalies.* Physical Review E, 2010. **81**(6): p. 061201.
20. Seth, J.R., L. Mohan, C. Locatelli-Champagne, M. Cloitre, and R.T. Bonnecaze, *A Micromechanical Model to Predict the Flow of Soft Particle Glasses.* Nature materials, 2011. **10**(11): p. 838.
21. Khabaz, F., T. Liu, M. Cloitre, and R.T. Bonnecaze, *Shear-Induced Ordering and Crystallization of Jammed Suspensions of Soft Particles Glasses.* Physical Review Fluids, 2017. **2**(9): p. 093301.
22. Khabaz, F., M. Cloitre, and R.T. Bonnecaze, *Particle Dynamics Predicts Shear Rheology of Soft Particle Glasses.* J. Rheol. (Submitted), 2019.
23. Krekelberg, W.P., V. Ganesan, and T.M. Truskett, *Shear-Rate-Dependent Structural Order and Viscosity of a Fluid with Short-Range Attractions.* Physical Review E, 2008. **78**(1): p. 010201.
24. Ingebrigtsen, T.S. and H. Tanaka, *Structural Predictor for Nonlinear Sheared Dynamics in Simple Glass-Forming Liquids.* Proceedings of the National Academy of Sciences, 2018. **115**(1): p. 87.
25. Ding, Y. and J. Mittal, *Equilibrium and Nonequilibrium Dynamics of Soft Sphere Fluids.* Soft Matter, 2015. **11**(26): p. 5274-5281.
26. Liu, T., F. Khabaz, R.T. Bonnecaze, and M. Cloitre, *On the Universality of the Flow Properties of Soft-Particle Glasses.* Soft Matter, 2018. **14**(34): p. 7064-7074.
27. Khabaz, F., M. Cloitre, and R.T. Bonnecaze, *Structural State Diagram of Concentrated Suspensions of Jammed Soft Particles in Oscillatory Shear Flow.* Physical Review Fluids, 2018. **3**(3): p. 033301.
28. Khabaz, F., T. Liu, M. Cloitre, and R.T. Bonnecaze, *Shear-Induced Ordering and Crystallization of Jammed Suspensions of Soft Particles Glasses.* Phys. Rev. Fluids, 2017. **2**(9): p. 093301.
29. Mohan, L., C. Pellet, M. Cloitre, and R. Bonnecaze, *Local Mobility and Microstructure in Periodically Sheared Soft Particle Glasses and Their Connection to Macroscopic Rheology.* J. Rheol., 2013. **57**(3): p. 1023-1046.
30. Seth, J.R., L. Mohan, C. Locatelli-Champagne, M. Cloitre, and R.T. Bonnecaze, *A Micromechanical Model to Predict the Flow of Soft Particle Glasses.* Nat. Mater., 2011. **10**(11): p. 838-843.
31. Liu, K.K., D.R. Williams, and B.J. Briscoe, *The Large Deformation of a Single Micro-Elastomeric Sphere.* J. Phys. D: Appl. Phys., 1998. **31**(3): p. 294.
32. Lees, A.W. and S.F. Edwards, *The Computer Study of Transport Processes under Extreme Conditions.* J. Phys. C: Solid State Phys., 1972. **5**(15): p. 1921-1928.
33. Plimpton, S., *Fast Parallel Algorithms for Short-Range Molecular Dynamics.* J. Comput. Phys., 1995. **117**(1): p. 1-19.
34. Larson, R.G., *The Structure and Rheology of Complex Fluids*. 1999, New York: Oxford Univ. Press.
35. Seth, J.R., M. Cloitre, and R.T. Bonnecaze, *Elastic Properties of Soft Particle Pastes.* Journal of rheology, 2006. **50**(3): p. 353-376.

36. Cloitre, M., R. Borrega, F. Monti, and L. Leibler, *Glassy Dynamics and Flow Properties of Soft Colloidal Pastes.* Physical Review Letters, 2003. **90**(6): p. 068303.
37. Khabaz, F., Cloitre, M. And Bonnecaze, R.T., *Particle Dynamics Predicts Shear Rheology of Soft Particle Glasses (in Review).* Journal of Rheology, 2020.
38. Dzugutov, M., *Dynamical Diagnostics of Ergodicity Breaking in Supercooled Liquids.* Journal of Physics: Condensed Matter, 1999. **11**(10A): p. A253-A259.
39. Mohan, L. and R.T. Bonnecaze, *Short-Ranged Pair Distribution Function for Concentrated Suspensions of Soft Particles.* Soft Matter, 2012. **8**(15): p. 4216-4222.

Supplementary Materials:
Excess Entropy Scaling for Soft Particle Glasses

Roger T. Bonnecaze[1*], Fardin Khabaz[1], Lavanya Mohan[1↓], Michel Cloitre[2]

[1]*McKetta Department of Chemical Engineering, The University of Texas at Austin, Austin, TX, 78712, USA*

[2]*Molecular, Macromolecular Chemistry, and Materials, ESPCI Paris, CNRS, PSL University, 10 Rue Vauquelin, 75005 Paris, France*

[*]Corresponding author electronic mail: rtb@che.utexas.edu

[↓]Current address: Exxon Mobil Upstream Research Company, 3120 Buffalo Speedway, Houston, TX 77098

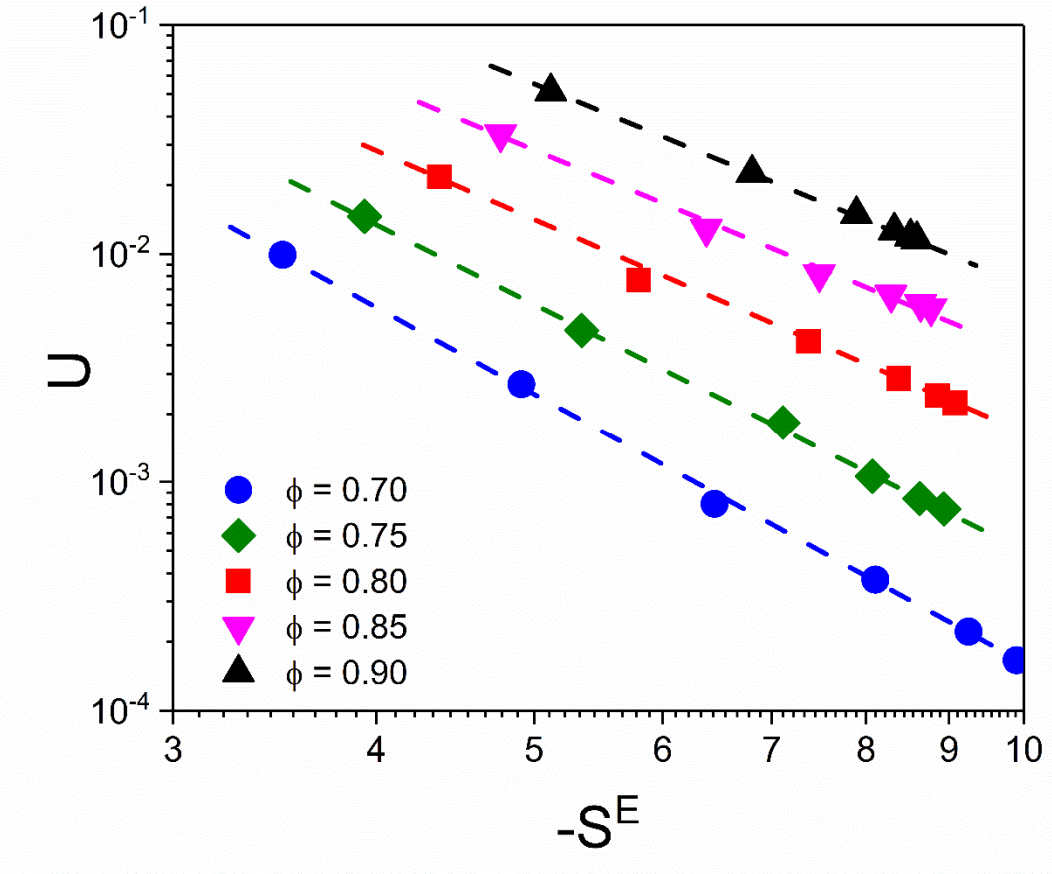

FIG S1. Elastic energy U as a function of the $-S^E$ for SPGs with different volume fractions. Dashed lines show power-law fits to the data.

Microstructural relaxation time:

We characterize the timescales that particles spend in their cage using the incoherent intermediate scattering function (ISF):

$$F_s(\mathbf{k},\tau)=\frac{1}{N}\left\langle \sum_{j=1}^{N}\exp\left[i\mathbf{k}\cdot\left(\mathbf{r}_j(\tau)-\mathbf{r}_j(0)\right)\right]\right\rangle, \tag{S1}$$

where $\mathbf{k}$ is a spatial wave vector and N is the total number of the particles in the simulation. We compute the ISF at different volume fractions and shear rates at a wave vector $kR = 4.0$, which is close to the position of the first peak of the structure factor and corresponds to the cage size. At all volume fractions, the decay of the ISF is nearly exponential, and we can determine a microstructure relaxation time τ_c from $F_s(k,\tau_c)=1/e$. See ref. [1] for details and discussion.

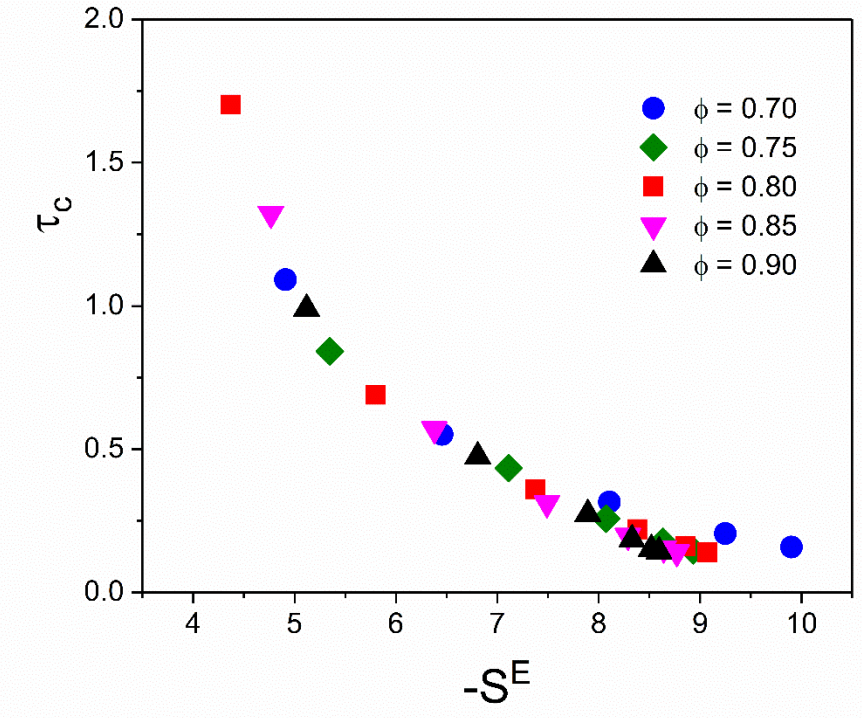

FIG S2. Microstructural relaxation time τ_c non-dimensionalized by the shear rate.

References

[1] Khabaz, F., M. Cloitre, and R.T. Bonnecaze, *Particle Dynamics Predicts Shear Rheology of Soft Particle Glasses.* J. Rheol. (submitted), 2019.